

Laminar forced convective heat transfer of Al_2O_3 /water nanofluids

A. M. Sharifi^{1,2}, A. Emamzadeh³, A. A. Hamidi⁴, H. Farzaneh¹
& M. Rastgarpour⁵

¹*Department of Environment and Energy, Science and Research Branch, Islamic Azad University, Tehran, Iran*

²*Zolal Iran Company, Iran*

³*Faculty of Management and Graduate School, Oil Industry University, Iran*

⁴*Faculty of Engineering, Tehran University, Iran*

⁵*Faculty of Engineering, Saveh Branch, Islamic Azad University, Iran*

Abstract

In this article, convective heat transfer of Al_2O_3 /water nanofluid was investigated using computational fluid dynamics (CFD). For this purpose the nanofluid was assumed as a single phase with temperature-dependent properties. The results of numerical modelling were evaluated by using experimental results. The results of both numerical and experimental investigations show that the convective heat transfer of base fluid (water) enhanced with increasing of Al_2O_3 nanoparticle concentration, fluid velocity and ethylene glycol concentration in the base fluid composition.

Keywords: nanofluid, forced convective heat transfer, Al_2O_3 nanoparticle, single phase model, temperature-dependent properties.

1 Introduction

Nanofluids are stable suspensions of nano-size particles in convectional fluids. These homogenous mixtures have enhanced thermal properties [1–3]. The results of experimental investigations show that the nanofluid convective heat transfer enhances with increasing of nanoparticles concentration (Table 1).

Choi [3] performed the first numerical study of nanofluid heat transfer in 1995. Single phase method is the first numerical technique has been used for



Table 1: The results of experimental investigations on nanofluid's heat transfer.

Author	Nanoparticles	Results
Heris <i>et al.</i> [5]	Al_2O_3	Maximum enhancement of 41%
Yang <i>et al.</i> [6]	Disc graphite	Maximum enhancement of 22%
Chen <i>et al.</i> [7]	titanate nanotube	Remarkable increasing of convective heat transfer with increasing of nanoparticles concentration and aspect ratio
Nguyen <i>et al.</i> [8]	Al_2O_3	Maximum enhancement of 40%
Ding <i>et al.</i> [9]	CNT	Remarkable enhancement of heat transfer coefficient

study of nanofluid convective heat transfer [10, 11]. In this method, nanofluid is assumed as a single phase without motion slip between nanoparticles and base fluid. Maiga *et al.* [12] and Palm *et al.* [13] have been employed single phase method for analysis of convective heat transfer of Al_2O_3 /water. Their results exhibit good agreement with the experimental results.

The relative velocity of nanoparticles and base fluid are considered in two phase method [14–16]. Behzadmehr *et al.* [17] employed this method for 1 Vol. % Cu nanofluid and reported that the turbulent convective heat transfer in a circular tube increased up to 15%. Bianco *et al.* [18] studied the forced laminar convection of nanofluid containing 100nm Al_2O_3 nanoparticles. They concluded that single phase and two phase methods exhibit approximated results, especially in the case of using temperature-dependent properties. Xuan and Roetzel [20] employed dispersion method for modeling of nanofluid thermal properties. They considered the chaotic movement of the nanoparticles in nanofluid, similar to dispersion theory in porous media proposed by Bear [21]. Mokmeli and Saffar-Avval [22] used dispersion method for analysis of the effect of volume fraction, average size of ATF-graphite and Al_2O_3 nanoparticles on the convective heat transfer of nanofluid.

The aim of this work is to study the forced laminar convective heat transfer coefficient of nanofluid containing Al_2O_3 nanoparticles. Single phase method with temperature-dependent properties is used for numerical simulation of nanofluid's thermal behaviour. Experimental investigations are used for validation of the results of numerical simulation.

2 Experimental

A design scheme of experimental set-up used at this work is shown in Figure 1. This system consists of a flow loop, pipeline system, a 25 litter reservoir tank, pumping and cooling system. Nanofluid flows through a horizontal copper tube with 1m length, 1 cm diameter and 1.7 mm thickness. The tube section is



insulated by using a layer of 25 mm of fiberglass, which is electrically heated at a constant rate of 5000 W/m^2 . The tube section is uniformly wound by Nickel-chrome wire connected to a DC 300 W power supply.

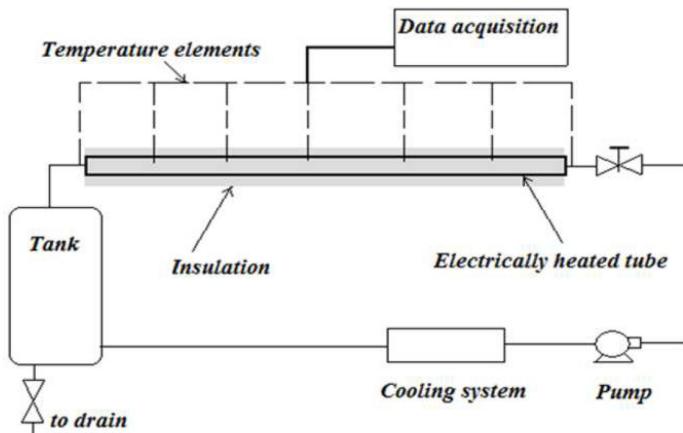


Figure 1: The experimental set-up.

Five K-type thermocouples are installed along the tube section and two K-type thermocouples are installed at the tube ends, for measuring of nanofluid bulk temperature. The local temperatures were transferred to a programmed computer system to calculate and store the Nusselt number and convective heat transfer coefficient (Eqs (1)–(3)). The nanofluid flow rate is measured by using a flow-meter, installed at tube entrance. The nanofluid flow rate and temperature are measured with uncertainties of 3% and 0.1. The nanofluid exits the tube section and is stored in a 25-liter tank, cooled and recycled to the tube section. Steady state condition is reached after 35 min. Cooling system consisted of a tubular heat exchanger, 50 cm in length which used cooling water for reducing the nanofluid temperature. The uncertainty of Re number and convective heat transfer coefficient were 3 and 6% in the experiments.

The nanofluid is prepared by addition of 10nm $\gamma\text{-Al}_2\text{O}_3$ nanoparticles (1–10 Vol. %) and 0.1 Vol. % Triton X-100 as stabilizer to distilled water as base fluid. The prepared mixture is homogenized by using an ultrasonic bath (model) for 10 hours. The produced stable nanofluid is used for thermal analysis. In the last step of experiments, for investigation of the effect of base fluid composition, ethylene glycol is mixed with water involving different volume concentrations (10, 20 and 40 Vol. %). The produced mixture is agitated in a flask and used for preparation of nanofluids. The Physical properties of Al_2O_3 nanoparticles (Nanostructured and Amorphous Materials, Inc, USA) are illustrated in tables 2 and 3 [23]. The thermal parameters (h_{ave} and Nu_{ave}) are estimated using equations (1)–(3). In these equations T_{local} , T_w and T_{input} are local temperature, wall temperature and input temperature, ρ and C_p and u are nanofluid density, specific heat and velocity, L and D are tube length and diameter and x is distance from tube inlet.

Table 2: The physical properties of ethylene glycol.

Molecular Formula	C2H6O2
Molar mass (kg·kmol ⁻¹)	62.07
Density (kg/m ³)	1113
Specific heat capacity (kJ·kg ⁻¹ ·K ⁻¹)	2.381
Viscosity (Pa·s)	0.02
Thermal conductivity(W·m ⁻¹ ·K ⁻¹)	0.256

$$h_{local} = \frac{(T_{local}-T_{input})\rho c_p u D}{4x(T_w-T_{input})} \quad (1)$$

$$h_{ave} = \frac{1}{L} \int_0^L h(z) dz \quad (2)$$

$$Nu_{ave} = \frac{h_{ave}.D}{K_{nf}} \quad (3)$$

3 Numerical studies

Single phase model was used for numerical simulation of convective heat transfer. The tube geometry is demonstrated in Figure 2. Nanofluid enters the tube at a uniform velocity (U_0) and temperature (T_0). At the end of the tube section, fully developed condition is assumed. The velocity and thermal fields of nanofluid are assumed symmetrical regarding to the centreline of the tube. The conservation equations for single phase method are illustrated below (Eqs. (4)–(7)) [24].

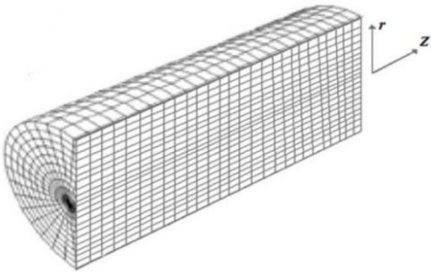


Figure 2: Geometrical configuration under study.

The physical properties of nanofluid are assumed as functions of physical properties of both base fluid and nanoparticles and their volume fraction (Eqs (8)–(11)) [18]. The physical properties of both nanofluid and base fluid were assumed temperature-dependent. The physical properties of base fluid were obtained by fitting a quadratic function on the NIST data for water (Eqs (12)–(15)) [25]. The viscosity of nanofluid is assumed as a function of nanoparticles size for ensuring more accurate results (Eq. (10)) [14].

The boundary conditions at the tube input is assumed relevant to the nanofluid input properties ($U=U_0$, $V=V_0$, $T=T_0$ and $P=P_0$) and the fully developed condition is assumed at the tube exit ($\frac{\partial}{\partial z} = 0$). No slip condition and constant heat flux were assumed at tube wall ($U=V=0$, $\frac{\partial p}{\partial r} = 0$, $q_w = \text{cte}$).

Table 3: The physical properties of γ -Aluminium Oxide Powder.

Average particle size (nm)	10
Specific surface area(m ² /g)	160
Purity (%)	99
Particle Morphology	Nearly spherical

Continuity equation:

$$\frac{\partial \rho}{\partial t} + (\nabla \cdot \rho \mathbf{U}) = 0 \quad (4)$$

Momentum equation:

$$\rho \frac{\partial \mathbf{U}}{\partial t} = -\nabla p + \mu \nabla^2 \mathbf{U} \quad (5)$$

Energy equation:

$$\rho C_p \frac{DT}{dt} = k \nabla^2 T \quad (6)$$

$$\frac{D}{Dt} = \frac{\partial}{\partial t} + (\mathbf{U} \cdot \nabla) \quad (7)$$

$$\rho_{nf} = (1 - \phi) \rho_{bf} + \phi \rho_{np} \quad (8)$$

$$C_{p,nf} = (1 - \phi) C_{p,bf} + \phi C_{p,np} \quad (9)$$

$$\mu_{nf} = \mu_{bf} + \frac{\rho_{np} \theta_g d_{np}^2}{72 \delta C} \quad (10)$$

$$\frac{k_{nf}}{k_{bf}} = 4.97 \phi^2 + 2.7 \phi + 1 \quad (11)$$

$$\rho_{bf} \left(\frac{kg}{m^3} \right) = -3.668 \times 10^{-3} T^2 - 6.867 \times 10^{-2} T + 1001, \quad T(^{\circ}C) \quad (12)$$

$$C_{p,bf} \left(\frac{J}{kg \cdot K} \right) = -7.798 \times 10^{-6} T^2 - 2.892 \times 10^{-4} T + 0.0124 \ln T + 4.224, \quad T(^{\circ}C) \quad (13)$$

$$\mu_{bf} (Pa \cdot s) = -5.051 \times 10^{-4} \ln(T + 2.459) + 2.567 \times 10^{-3}, \quad T(^{\circ}C) \quad (14)$$

$$k_{bf} \left(\frac{W}{m \cdot K} \right) = -9.751 \times 10^{-6} T^2 - 2.163 \times 10^{-3} T + 0.5596, \quad T(^{\circ}C) \quad (15)$$

Several non-uniform grids have been tested for ensuring that the model results are grid independent (100×125, 200×250, 400×500, 800×1000). The accuracy of model results increases by increasing the number of grids up to 200×250 nodes along the radial and axial directions (the thermal field was assumed symmetrical regarding the tube centreline using no tangential). No significant enhancement has been observed after this point. The non-uniform

grids including 200×250 nodes have been used. The number of nodes near to tube wall is higher.

The conservation equations for steady state conditions in two-dimensional system were discretized using finite difference method. Matlab version R2010a was used for computational processing (implemented by a 3 GHZ Intel Core i5 Duo CPU processor with 4 GB RAM) of numerical model. The first trial values for the operational variables are illustrated in table 4. The intended convergence for velocity, temperature and pressure are 10^{-5} m/s, 0.01°C and 1 Pa respectively.

Table 4: First trial values for operational variables.

Parameter	Initial value
Axial velocity (U)	Nanofluid inlet velocity (U_0)
Radial velocity (v)	0
Temperature (T)	Nanofluid inlet temperature (T_0)
Pressure (P)	Nanofluid inlet pressure with 1% loss along the tube $P_i = P_0(1 - 0.01Z/L)$; Z=distance from tube inlet, L=tube length

The model was employed for comprehensive analysis of the effects of Al_2O_3 concentration (0, 1, 2, 5 and 10 Vol. %), Reynolds number (250–500 and 1000), nanofluid inlet temperature (20, 30, 40 and 60°C) and base fluid composition (0, 10, 20, 30 and 40 Vol. % of EG).

4 Model validation

The results of Numerical simulation were initially validated by implementing of model and experimental investigation for the forced convection heat transfer of pure water flows ($\text{Re}=250$) through a horizontal tube exposed to constant heat of 5000 W/m^2 . As can be seen in table 5, the results of model are in good agreement with experimental results. According to the Perry's handbook, the Values of limiting Nusselt number in laminar flow in closed ducts is 4.36 [23].

Table 5: The results of model and experimental investigations for pure water.

Thermal properties	Model results	Experimental results
Nu_{av}	4.37	4.51
h_{av}	261.81	272.31

5 Results and discussions

5.1 The effect of Al_2O_3 nanoparticles concentration

The nanoparticles concentration was varied between 1 and 10 Vol. %. The convective heat transfer of nanofluid ($h_r = h_{\text{nanofluid}} / h_{\text{base fluid}}$) is shown in Figure 3. The temperature and velocity fields of nanofluid containing 5 Vol. % Al_2O_3 nanoparticles are shown in Figures 4 and 5. The forced convective heat

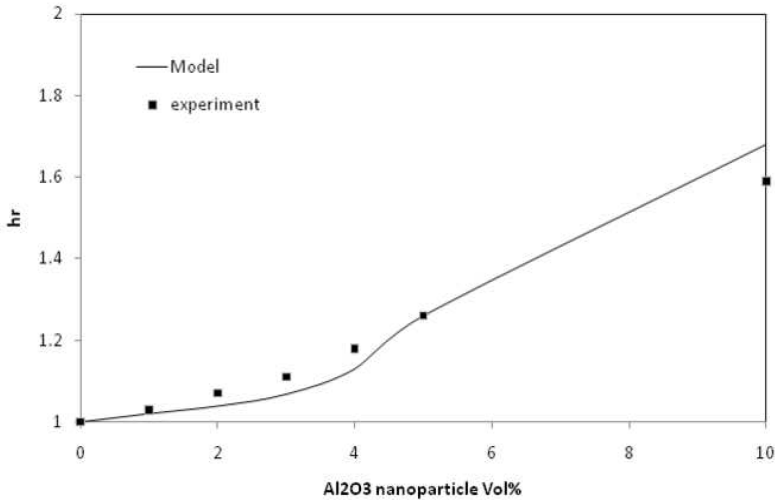


Figure 3: The effect of Al_2O_3 nanoparticles concentration on the convective heat transfer coefficient of nanofluid at $\text{Re}=250$ and $q_w=5000 \text{ W/m}^2$.

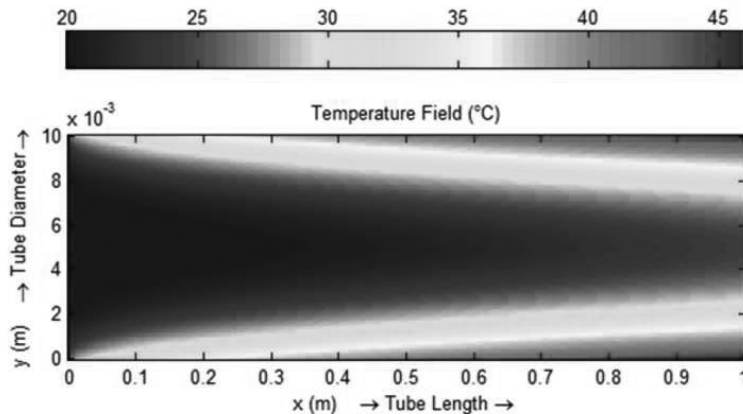


Figure 4: The temperature field of nanofluid flow, contains 5 Vol. % Al_2O_3 at $\text{Re}=250$, $T_0=20^\circ\text{C}$ and $q_w=5000 \text{ W/m}^2$.

transfer coefficient increases with increasing of nanoparticles concentration. The convective heat transfer coefficient of nanofluid containing 5 Vol. % Al_2O_3 was observed 27% higher than water. At similar operating conditions, the fluids with higher conductive heat transfer coefficient have higher convective heat transfer coefficient. The thermal conductivity of nanofluid is a function of thermal conductivity of both base fluid and nanoparticles. Increasing of nanoparticles concentration, results in increasing of conductive heat transfer coefficient and consequently convective heat transfer [18].

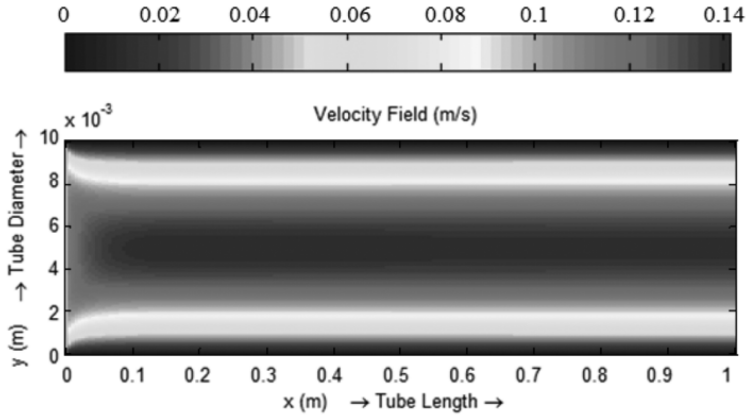


Figure 5: The velocity field of nanofluid flow contains 5 Vol. % Al_2O_3 at $\text{Re}=250$, $T_0= 20^\circ\text{c}$ and $q_w=5000 \text{ W/m}^2$.

5.2 The effect of nanofluid flow Reynolds number

The effect of Re number on the heat transfer is illustrated in Figure 6. The velocity and temperature fields of nanofluid flows at $\text{Re}=1000$ are demonstrated in Figures 7 and 8. The forced convective heat transfer increases with increasing of nanofluid flow Reynolds number. Increasing of flow Reynolds number, results in increasing of turbulent eddies. This event causes increasing of effective thermal conductivity of nanofluid and consequently increasing of convective heat transfer [26].

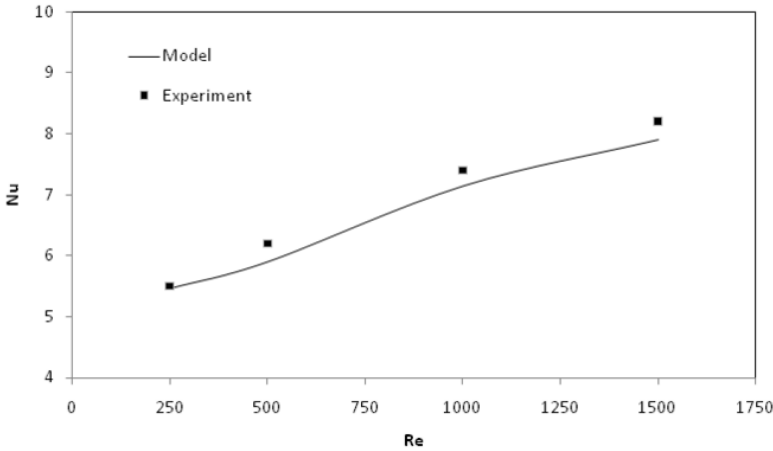


Figure 6: The effect of nanofluid flow Reynolds number on the Nusselt number at 5 Vol. % of Al_2O_3 nanoparticles and $q_w=5000 \text{ W/m}^2$.

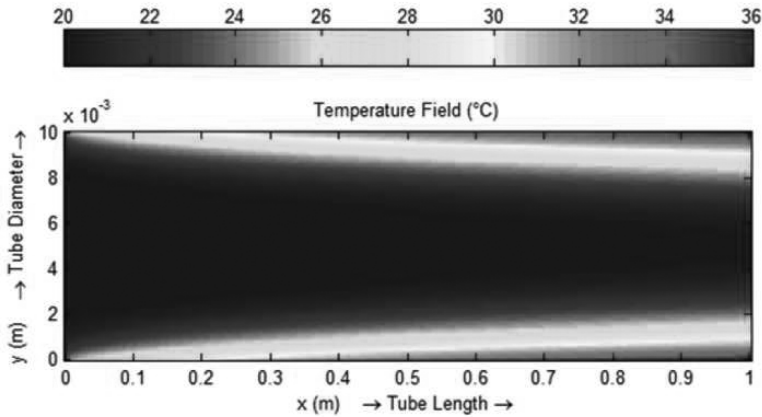


Figure 7: The temperature field of nanofluid flow at $Re=1000$, 5 Vol. % of Al_2O_3 nanoparticles and $q_w=5000 \text{ W/m}^2$.

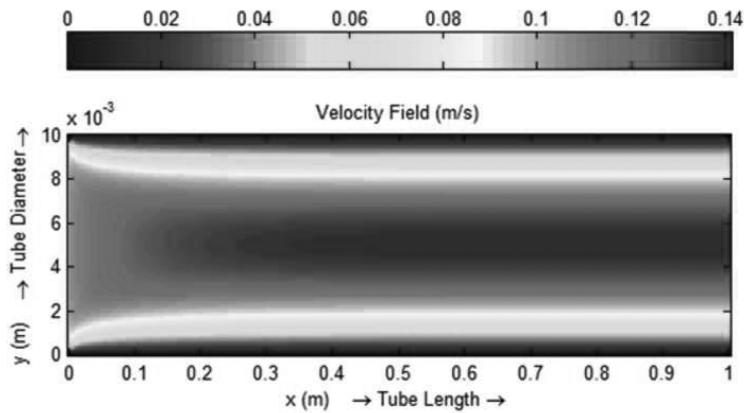


Figure 8: The velocity field of nanofluid flow at $Re=1000$, 5 Vol. % of Al_2O_3 nanoparticles and $q_w=5000 \text{ W/m}^2$.

5.3 The effect of nanofluid input temperature

As can be seen in Figure 9, similar to conventional fluids the convective heat transfer coefficient of nanofluid increases with increasing of input temperature. This may be due to increasing of Brownian motions of nanoparticles. Similar results have been reported by Koblinski *et al.* [27].

5.4 The effect of base fluid composition

The effect of EG concentration in the base fluid composition on the nanofluid heat transfer coefficient was investigated. As can be observed in Figure 10,

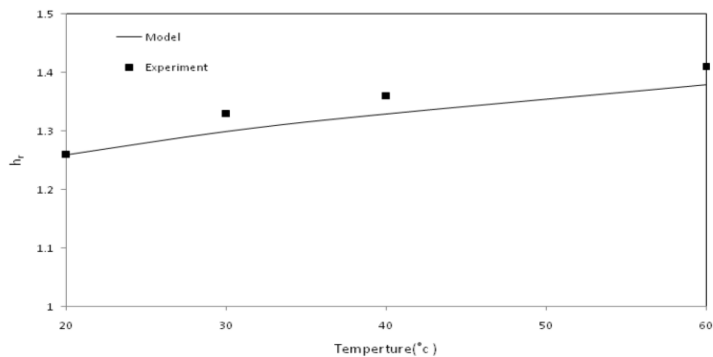


Figure 9: The effect of nanofluid input temperature on the convective heat transfer coefficient at $Re=250$, 5 Vol. % of Al_2O_3 nanoparticles and $q_w=5000 \text{ W/m}^2$.

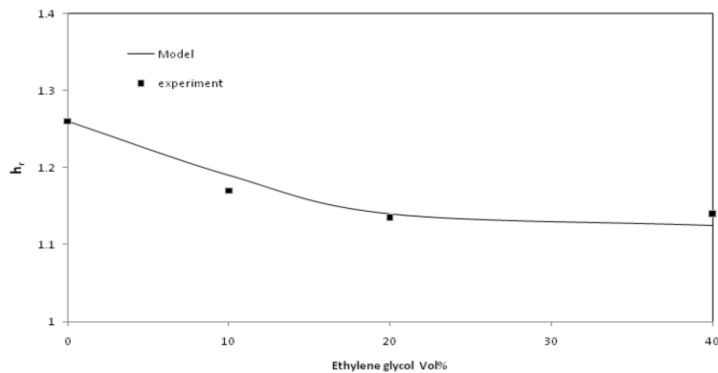


Figure 10: The effect of EG concentration in the base fluid composition on the convective heat transfer coefficient at $Re=250$, 5 Vol. % of Al_2O_3 nanoparticle and $q_w=5000 \text{ W/m}^2$.

increasing of EG concentration in the base fluid composition results in decreasing of convective heat transfer. Ethylene glycol has lower conductivity regarding the water (K_{water} at $20^\circ\text{C} = 0.58 \text{ W}\cdot\text{m}^{-1}\cdot\text{K}^{-1}$) [23] and increasing of its concentration in the EG/water mixture, results in increasing of base fluid conductivity and consequently enhancement of nanofluid convective heat transfer [28].



6 Conclusions

Numerical simulation and experimental investigation were employed for study of laminar forced convective heat transfer of nanofluid containing 10nm Al_2O_3 nanoparticles at constant heat flux. The results of both numerical and experimental investigations indicate that the convective heat transfer of water increased significantly by adding Al_2O_3 nanoparticles. The convective heat transfer of nanofluid increases with increasing of nanoparticle concentration, Reynolds number and inlet temperature. Increasing of EG concentration in the base fluid composition, results in decreasing of nanofluid convective heat transfer coefficient. Increasing of flow Reynolds number results in later formation of fully developed region and decreasing of tube wall temperature.

Acknowledgements

This work was supported in part by the Zolal Iran Company (EPC Contractor in Water and Wastewater Treatment), Tehran, Iran. The first author would thank the Zolal Iran Company.

References

- [1] Eastman, J. A., Choi, U. S., Li, S., Thompson, L. J., and Lee, S., "Enhanced Thermal Conductivity through the Development of Nanofluids Y Proc. of the Symposium on Nanophase and Nanocomposite Materials H, Materials Research Society, Boston, Vol. 457, pp. 3-11, 1995.
- [2] Stephen U. S. Choi, Energy technology division, Argonne national laboratory, Northern Illinois University, January 15, DeKalb, IL, 2005.
- [3] Choi, U. S., "Enhancing Thermal Conductivity of Fluids with Nanoparticles, Developments and Applications of Non-Newtonian Flows, eds. D. A. Siginer and H. P. Wang, The American Society of Mechanical Engineers, New York, FED 23 VM.D, VO1.66, pp. 99-105, 1995.
- [4] Eastman, J.A., Mechanisms of Enhanced Heat Transfer in Nanofluids, Materials Science Division, Argonne National Laboratory, Fluctuations and Noise in Out of Equilibrium Systems, Sep 14-16, 2005.
- [5] Zeinali Heris, S., Nasr Esfahany, Etemad, M. S. Gh., Experimental investigation of convective heat transfer of Al_2O_3 /water nanofluid in circular tube International Journal of Heat and Fluid Flow, Vol.28, pp. 203–210, 2007.
- [6] Yang Y, Zhang ZG, Grulke EA, Anderson WB, Wu G. Heat Transfer Properties of Nanoparticle-in-Fluid Dispersions (Nanofluids) in Laminar Flow. Int J Heat Mass Transfer, Vol.48, No.6, pp. 1107–1116, 2005.
- [7] Chen, H., Yang W., He, Y., Ding, Y., Zhang, L., Tan, C., Lapkin, A., Bavykin, V. D., Heat transfer and flow behavior of aqueous suspensions of titanate nanotubes (nanofluids), Powder Technology Vol.183, pp. 63–72, 2008.



- [8] Nguyen, C. T., Roy, G., Gauthier, C., Galanis, N., Heat transfer enhancement using Al_2O_3 -water nanofluid for an electronic liquid cooling system, *Applied Thermal Engineering*, Vol.27 pp. 1501–1506, 2007.
- [9] Ding, H. Alias, D. Wen, R.A. Williams, Heat transfer of aqueous suspensions of carbon nanotubes (CNT nanofluids), *International Journal of Heat and Mass Transfer* Vol.49 No.1 pp. 240–250, 2005.
- [10] Choi S, Zhang Z, Yu W, Lockwood F, Grulke E. Anomalous thermal conductivity enhancement of in nanotube suspensions. *Applied Physics Letters*, Vol.79 No.14, pp. 2252– 2254, 2001.
- [11] Pak, B.C., Cho, Y.I., Hydrodynamic and heat transfer study of dispersed fluids with submicron metallic oxide particles. *Experiment. Heat Transfer*, Vol.11, No.2, pp. 151–170, 1998.
- [12] Maiga, S. B., Palm, S. J., Nguyen, C. T., Roy, G., Galanis, N., Heat transfer enhancement by using nanofluids in forced convection flows, *International Journal of Heat and Fluid Flow*, Vol.26, pp. 530–546, 2005.
- [13] Palm, S. J., Roy, G., Nguyen C. T., Heat transfer enhancement with the use of nanofluids in radial flow cooling systems considering temperature-dependent properties. *Applied Thermal Engineering* Vol.26, No.17–18, pp. 2209–2210, 2006.
- [14] Izadi, M., Behzadmehr, A. D., Jalali, V., Numerical study of developing laminar forced convection of a nanofluid in an Annulus, *International Journal of Thermal Sciences*, Vol.48 2119–2129, 2009.
- [15] Lotfi, R., Saboohi, Y., Rashidi, A.M., Numerical study of forced convective heat transfer of Nanofluids: Comparison of different approaches, *International Communications in Heat and Mass Transfer* Vol.37, pp. 74–78, 2010.
- [16] Mirmasoumi, S., Behzadmehr, A., Effect of nanoparticles mean diameter on mixed convection heat transfer of a nanofluid in a horizontal tube, *International Journal of Heat and Fluid Flow* Vol.29, pp. 557–566, 2008.
- [17] Behzadmehr, M., Saffar-Avval, N., Galanis, Prediction of turbulent forced convection of a nanofluid in a tube with uniform heat flux using a two phase approach, *International Journal of Heat and Fluid Flow* Vol.28, pp. 211–219, 2007.
- [18] Bianco, V., Chiacchio, F., Manca, O., Nardini, S., Numerical investigation of nanofluids forced convection in circular tubes, *Applied Thermal Engineering*, Vol.29, pp. 3632–3642, 2009.
- [19] Yurong, H., Yubin, M., Yunhua, Z., Huilin, L., Yulong, D., Numerical investigation into the convective heat transfer of TiO_2 nanofluids flowing through a straight tube under the laminar flow conditions, *Applied Thermal Engineering*, Vol.29, pp. 1965–1972, 2009.
- [20] Xuan, Y., Roetzel, W., Conceptions for heat transfer correlation of nanofluids, *Int. J. Heat Mass Transfer* Vol.43, pp. 3701–3707, 2003.
- [21] Bear, J., *Dynamics of Fluids in Porous Media* Second printing. American Elsevier Publishing Company, 1975.



- [22] Mokmeli, A., Saffar-Avval, M., Prediction of nanofluid convective heat transfer using the dispersion model, *International Journal of Thermal Sciences*, Vol.49, pp. 471–478, 2010.
- [23] Perry, R. H., Green, D. W., *Perry's chemical engineers' handbook*; 7th edition, McGraw-Hill, New York, 1997.
- [24] Bird, R.B., Stewart, W.E., Lightfoot, E.N., *Transport Phenomena*; 2nd edition, John Wiley & Sons, Inc., New York, 2002.
- [25] <http://webbook.NIST.gov/chemistry/fluid> (2010).
- [26] Xuan, Y., Li, Q., Heat transfer enhancement of nanofluids. *International Journal of Heat and Fluid Flow*, Vol.21, pp. 58–64, 2000.
- [27] Keblinski, P., Phillpot, S. R., Choi, S. U. S., Eastman, J. A., Mechanisms of heat flow in suspensions of nano-sized particles (nanofluids), *International Journal of Heat and Mass Transfer*, Vol.45, pp. 855–863, 2002.
- [28] Al-Amayreh, M., Experimental Study of Thermal Conductivity of Ethylene Glycol Water Mixtures, Vol.44, No.2, pp. 300-313, 2010.

